

Buckling and Failure of Flat Stiffened Panels

S. Yusuff*

West Virginia University, Morgantown, W. Va.

Compression panels, regardless of the local buckling of the skin, can be divided into three regions: short panels, having slenderness ratio equal to or less than 10, long panels, which are shown to fail essentially because of the long wave buckling of the skin, and panels of intermediate length in the transition region. In this paper, a comprehensive and self-sufficient analysis is presented for computing the failing stresses of stiffened panels, in particular, Z-section stiffened panels, in all possible regions of interest. The analysis not only includes the review of the methods previously proposed, but also comprises of many new results, such as the author's most recent formulas based on energy methods for the short and long wave buckling of the skin, the development of the formulas for the maximum strength of panels, and the application of the power law for determining the strength of the panels in the transition range. Since numerous types of panels and modes of failure are involved, the methods of analysis naturally are complex. Therefore, for the clarification of the various steps involved in the computations and for the removal of the confusion that may arise in the minds of the readers, adequate examples are included wherever needed. Extensive comparison of the analysis also is made with tests on 75S-T6 and 24S-T aluminum Z-stiffened panels. It is shown that the analysis is in good agreement with tests.

Nomenclature

A_s	= stiffener area
b	= stiffener spacing
b_e	= effective width of sheet
B, C	= parametric constants
D	= flexural rigidity of plate of unit width { $Et^3/[12(1-\nu^2)]$ }
d_A	= attached flange width
d_F	= outstanding flange width
E	= Young's modulus
G	= shear modulus
h	= height of stiffener
H	= develop width of stiffener ($=h+d_F+d_A$)
I_s	= moment of inertia of stiffener about its own centroid
I_e	= effective moment of inertia of stiffener
J	= torsional constant
l	= pin-ended length of panel
m	= number of half-waves across l
t	= thickness of skin
t_s	= thickness of stiffener
\bar{Y}_s	= distance between centroid of stiffener and median line of skin
σ_{cr}	= critical compression stress
σ_e	= edge stress
σ_{tr}	= transition stress
σ_f	= failing stress
$\bar{\sigma}_f$	= average failing stress
$\sigma_{m,0}$	= maximum stress of stiffened panel at $l/\rho=0$
$\sigma_{m,10}$	= maximum stress of stiffened panel at $l/\rho=10$
σ_{cy}	= yield stress of material in compression
β	= constant
ρ	= radius of gyration of skin-stiffener element with skin fully effective
ρ'	= radius of gyration of stiffener with effective skin
l/ρ	= slenderness ratio
$(l/\rho)_{tr}$	= transition slenderness ratio
ν	= Poisson's ratio

ϕ	= $m\pi b/l$
ψ	= buckling parameter ($=b(t\sigma_{cr}/D)^{1/2}$)
μ	= ratio of bending rigidity of plate of width b to torsional rigidity of stiffener ($=bD/JG$)
η	= plasticity correction

Introduction

THE buckling and failure of stiffened panels are complex problems encountered in the design of stiffened construction such as wing surfaces subjected to compression loads. Because there are many dimensional parameters and different modes of buckling to be considered, the determination of the strength of panels and the selection of the most efficient panel are challenging problems, which require skill and considerable experience on the part of structural engineers. In spite of extensive studies, the design of stiffened panels in actual practice is not based on theoretical solutions alone. Very often test data and the design charts,¹⁻³ prepared on the basis of data, also are used.

In the following, a rational analytical analysis, which is self-sufficient and comprehensive, is presented for computing the failing stresses of flat stiffened panels. Because of the high efficiency and advantages due to simplicity in shape and construction, and because of the need to clarify the mechanism of failures and to explain how the methods of analysis are devised, Z-section stiffened panels are considered herein. It is assumed that the stiffeners are extruded or formed, and that the pitch and the diameters of rivets used in the construction of panels are such that they yield the potential strength of the panels. Hence, the stiffened panels are considered to be monolithic.

In Z-section stiffened panels, the various dimensional parameters involved are t_s/t , b/t , h/t_s , d_f/t_s , d_A/t_s (Fig. 1) and l/ρ . The panels are assumed to be simply supported at the ends, and the sides are unsupported. In tests done in NACA on stiffened panels, the panels were tested flat-ended and the end-fixity coefficient was identified to be equivalent to 3.75. Herein, however, such panels are assumed to be clamped, and hence assumed to have an end-fixity coefficient of 4. Consideration of the compressive strength of panels can be divided into three regions: short panels, having slenderness ratio $l/\rho=10$, that are assumed to attain the maximum strength, sometimes called the crippling strength; long panels in which skin (plate, or sheet) buckling is shown to occur in long wave, with one buckle across the simply supported ends—the failure being coincident with this buckling; and

Presented as Paper 74-409 at the AIAA/ASME/SAE 15th Structures, Structural Dynamics and Material Conference, Las Vegas, Nev., April 17-19; submitted Apr. 18, 1974; revision received July 18, 1975.

Index categories: Structural Stability Analysis; Structural Design, Optimal.

*Professor of Aerospace Engineering. Associate Fellow AIAA.

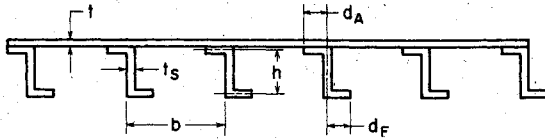


Fig. 1 Cross section of Z-stiffened panels.

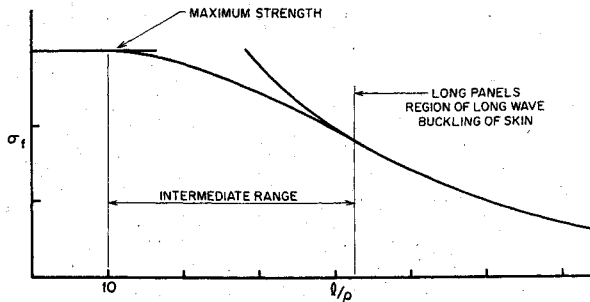


Fig. 2 Strength of stiffened panels.

finally the panels of intermediate length (see Fig. 2) belonging to transition range in which the column effect is significant. Panels in each of these regions can be further classified in two types: panels subjected to local buckling of the skin, and panels in which skin does not buckle locally before failure. The methods of analysis presented herein are for computing the failing stresses of panels in all the regions over a wide range of dimensional parameters. The analysis therefore is comprehensive and comprised of many new results, and also is a review of methods previously proposed. The analysis is illustrated by examples, and also is compared with extensive available data on 75S-T6 aluminum alloy panels having Z-section stiffeners, which are either formed or extruded. The comparison of analysis with tests is shown to be excellent.

Short Wave or Local Buckling of Skin

As noted earlier, stiffened panels belonging to each of the three regions mentioned previously can be classified into two types with respect to the short wave or local buckling of the skin. The stresses at which the sheet buckles locally should be known for calculating the effective width of the buckled sheet and for designing the wing surfaces, which retain smooth and unbuckled surface up to high values of applied load. In Ref. 4, Gallaher and Boughan have presented charts for calculating the buckling coefficient for an idealized Z-stiffened plate. For the type of buckling which commonly occurs in Z-section stiffened panels, charts presented in Refs. 5 and 6 are quite general; the local buckling stress can be obtained quickly, without any idealization, except that the stiffeners are regarded as "sturdy" (they do not buckle in their own cross sectional planes). In Ref. 6, the author has shown that the stresses obtained from the chart given therein is in excellent agreement with tests. One or two exceptions are pointed out later on in this section.

Recently, the author has investigated,⁷ by the energy method, the local instability of the plate whose sides are subjected to the torsional restraining effects of sturdy stiffeners. The solution, Eq. (6) of Ref. 7, is the following quadratic equation:

$$(\psi^2)^2 - \beta\psi^2 + c = 0 \tag{1}$$

where

$$B = \pi^2 \left\{ \left[\frac{mb}{\ell} + \frac{\ell}{mb} \right]^2 + \left[\frac{mb}{\ell} + \frac{4\ell}{mb} \right]^2 + \frac{10}{\mu} \right\}$$

$$C = \pi^4 \left\{ \left[\frac{mb}{\ell} + \frac{\ell}{mb} \right]^2 \left[\frac{mb}{\ell} + \frac{4\ell}{mb} \right]^2 + \frac{8}{\mu} \left[\frac{mb}{\ell} + \frac{\ell}{mb} \right]^2 + \frac{2}{\mu} \left[\frac{mb}{\ell} + \frac{4\ell}{mb} \right]^2 \right\}$$

and, for Z-stiffened panels,

$$\mu = 0.715 (b/t) (t_s/h) (t/t_s)^4$$

For a given value of μ and ℓ/b , assume $m=1,2,3$, etc., and then compute ψ from Eq. (1). The actual value of m that is valid is that which corresponds to a minimum value of ψ . Using the minimum value of ψ thus obtained, the critical stress for the local or short buckling mode is obtained from

$$\frac{\sigma}{\eta} = \frac{E\psi^2}{12(1-\nu^2)} \left(\frac{t}{b} \right)^2 \tag{2}$$

Equation (1) is in excellent agreement with the chart (Fig. 5 of Ref. 6) and also, as shown in Ref. 7, with the extensive test data. Therefore, either of these two results can be used to yield accurate local buckling stresses. However, it may be mentioned here that the author has noted that the computed buckling stress differs from that of test for the panel having the configuration $t_s/t=1$, and $b/t=h/t_s=30$. The tests indicate that for this panel the torsional restraining effect of the stiffeners on the sides of the sheet is negligibly small and the local buckling of the sheet occurs as if the sides are simply supported. Therefore, for the previous configuration, ψ has the value 6.28 corresponding to the simply supported condition.

Maximum Strength of Stiffened Panels

The maximum strength, sometimes known as the crippling strength, of a stiffened panel, is the failing stress of a panel having a slenderness ratio of 10 if the ends of the panel are simply supported. Since this stress determines the upper limit, the formula for determining this stress for any given cross-sectional configuration of a panel is highly important for the designers. Gerard^{8,9} has proposed the following formula for the maximum strength of stiffened panels

$$\frac{\bar{\sigma}_f}{\sigma_{cy}} = \beta \left[g \frac{t_s t}{A_s + bt} \left(\frac{E}{\sigma_{cy}} \right)^{1/2} \right]^m \tag{3}$$

For Z-stiffened panels, $m=0.85$ is used. For the remaining two constants either of the following two pairs of values, $\beta=0.56$, $g=7.83$ or $\beta=1.26$, $g=3$, which yield identical results, are recommended. By use of the first set of values, Eq. (3) for Z-stiffened panels can be written as follows:

$$\frac{\bar{\sigma}_f}{\sigma_{cy}} = 0.56 \left[\frac{7.83}{\left(\frac{H}{t_s} \frac{t_s}{t} + \frac{b}{t} \frac{t}{t_s} \right)} \left[\frac{E}{\sigma_{cy}} \right]^{1/2} \right]^{0.85} \tag{4}$$

In this equation the designer can see directly the various non-dimensional variables involved in the formula. By use of this formula, the maximum strengths of some 75S-T6 aluminum alloy Z-stiffened panels are computed. The computed values together with the test results are listed in Table 1. It can be seen that, even though Gerard's formula is in good agreement in many cases, it is also in serious error with many other cases. Therefore, the author found it necessary to formulate a new method for obtaining the maximum strength of Z-stiffened panels. The proposed method is as follows.

The critical dimensions for Z-stiffeners attached to a sheet are t_s , h , and d_f . Since the other flange is attached to the sheet, its width is not considered to be critical. The highest

stress (uniform or average) that Z-stiffener attached to the sheets can sustain is assumed to be given by

$$\frac{\bar{\sigma}}{\sigma_{cy}} C = \left[\frac{t_s}{h+d_f} \left(\frac{E}{\sigma_{cy}} \right)^{1/3} \right]^{0.75} \quad (5)$$

where $C=3.2$ for 75S-T6 aluminum alloy and $C=3.8$ for 24S-T aluminum alloy stiffener. This formula, and the effects of other dimensions b and t of the sheet-stiffener element, are considered in the following manner for getting the maximum strength of stiffened panels.

If the sheet does not buckle locally, the strength of the panel is assumed to be the same as the strength of stiffener attached to sheet. In panels having small b/t , since the sheet does not buckle before failure, the sheet and stiffener are assumed to be uniformly stressed, and the failure of the panels occurs when the uniform stress corresponds to the crippling strength of the stiffener on its own. Hence, the maximum strength of such panels is computed from Eq. (5). If, on the other hand, the sheet buckles early, as in the case of panels having large b/t , the panels do not fail immediately. They continue to sustain greater loads until the stress in the stiffener is increased to its maximum strength on its own. With this stress of the stiffeners regarded as the edge stress for the buckled sheet, the effective width of the sheet is computed. For calculation of the effective width, the following two formulas are considered: Von Karman's formula,

$$b_e/b = (\sigma_{cr}/\sigma_e)^{1/2} \quad (6)$$

and Marguerre's formula

$$b_e/b = (\sigma_{cr}/\sigma_e)^{1/3} \quad (7)$$

where b_e is the effective width of the sheet associated with a stiffener at the midpoint of b_e , σ_{cr} is the local buckling stress, and σ_e is the edge stress, as given by Eq. (5).

The effective width, in addition to depending upon critical stresses as in the previous equation, also depends upon the ratio A_s/bt . Equation (6) is recommended for $A_s/bt > 0.4$, and Eq. (7) for $A_s/bt \leq 0.4$ for calculating the effective width. Then the maximum strength of panel is obtained from

$$\begin{aligned} \bar{\sigma}_f &= \frac{A_s + b_e t}{A_s + bt} \sigma_e = C \sigma_{cy} \frac{A_s + b_e t}{A_s + bt} \\ &\times \left[\frac{t_s}{h+d_f} \left(\frac{E}{\sigma_{cy}} \right)^{1/3} \right]^{0.75} \quad (8) \end{aligned}$$

The strength of panels computed from the aforementioned method is given in Table 1. It can be seen that these values are in better overall agreement with tests than those obtained from Gerard's formula. Furthermore, because of simplicity, the present method has other advantages from the design point of view, as illustrated by the following example.

Calculate the cross-sectional configuration of Z-stiffened panel that can attain the stress equal to the yield stress (76.9 ksi) of 75S-T6 aluminum alloy. From Eq. (5), we obtain that $(h+d_f)/t_s$ must be equal to 24 for $\bar{\sigma}_f = 76.9$ ksi. Since the outstanding flange d_f is generally equal to $0.4h$, the h/t_s should be less than or equal to 17.1. The appropriate value of b/t from efficiency consideration should correspond to local buckling of the skin at 76.9 ksi. The required b/t can be obtained from Eq. (2) by use of the following data.

At yield stress, $\sigma_{cr}/\eta = 100$ ksi for 75S=T6 aluminum alloy,¹⁰ $\psi = 7.6$ for b/t close to h/t_s , and $t_s/t = 1$, from Eq. 5 of Ref. 6. Substituting these data in Eq. (2), we have b/t equal to 21.6. The required cross-sectional parameters for attaining the yield stress of 75S-T6 aluminum alloy Z-stiffened panel should be, for $t_s/t = 1$, $h/t_s \leq 17.1$, $b/t \leq 21.6$, and $\ell/\rho = 10$. From the test¹¹ it is seen that the panel having the con-

figuration $t_s/t = 1$, $b/t = 20$, $h/t_s = 12.6$ and $\ell/\rho = 10$ attained 75.2 ksi for the 75S-T6 aluminum alloy Z-stiffened panel. This result not only confirms the present method, but also indicates the approach for obtaining the most efficient design. Further comparison of the theory with tests is made in Figs. 3-7. The test data used in these figures deal with two aluminum alloy panels in which b/t varies from 20 to 75, h/t_s varies from 20 to 50, and t_s/t varies from 1.0 to 0.63. Note that up to the buckling of the sheet the maximum strength of the panels remains constant, as envisaged herein, as b/t varied for the same h/t_s . It can be seen that the agreement between the tests and the present analysis is excellent over such a wide range of dimensional parameters.

Failure and Strength of Long Panels

In the preceding section, the compressive strength of panels having slenderness ratio $\ell/\rho = 10$ has been established. Now it is pertinent to consider the strength of panels of various lengths. In this section we are interested in long panels having slenderness ratio greater than 40 if they are unbuckled; however, if the skin buckles locally, long panels are considered to be those that have slenderness ratio greater or equal to 62.5. These two types of panels lie to the right of the transition range (Fig. 2). They are considered as follows.

Long Panels with no Local Buckling of Skin

Below the local buckling stress of the skin, the panel is treated⁸ as a column, and the following Euler formula is used for calculating the failing stresses:

$$\frac{\sigma_f}{\eta} = \frac{\pi^2 EI_E}{\ell^2 (A_s + bt)} = \frac{\pi^2 E}{(\ell/\rho)^2} \quad (9)$$

The author⁶ has shown that this formula is not in agreement with test data, and that it can be in error as much as 30%. In addition, the failure of panels is caused by the long wave ($m=1$) buckling of the sheet as given by Eq. (13) of Ref. 6, which is a transcendental equation: this equation represents the buckling of sheet that is elastically supported by stiffeners, with each stiffener having an effective moment of inertia I_e , which is to be evaluated as shown in the following. This equation is shown⁶ to be in excellent agreement with Z sections and integrally machined unflanged stiffeners. The author recently has investigated the long wave buckling of the skin by the energy method. For long panels the following results are taken from this unpublished work.

The buckling parameter ψ for long panels can be obtained from

$$A(\psi^2)^2 - B\psi^2 + c = 0 \quad (10)$$

where

$$A = 0.2356(A_s/bt) + 0.0426$$

$$\begin{aligned} B &= \left(\phi + \frac{1}{\phi} \right)^2 \left(1.075 \frac{A_s}{bt} + 2.6786 \right) \\ &+ \left(\phi + \frac{4}{\phi} \right)^2 \left(2.2407 \frac{A_s}{bt} + 2.6786 \right) \\ &- \left(\phi + \frac{1}{\phi} \right) \left(\phi + \frac{4}{\phi} \right) \left(3.08 \frac{A_s}{bt} + 5.2736 \right) \\ &+ 0.2356 \frac{EI_e}{bD} \phi^2 \times (1-\nu) 4.258 \end{aligned}$$

and

$$\begin{aligned} C &= 0.0418 \left(\phi + \frac{1}{\phi} \right)^2 \left(\phi + \frac{4}{\phi} \right)^2 + \left(\phi + \frac{1}{\phi} \right)^2 [1.075 \\ &\times \frac{EI_e}{bD} \phi^2 - (1-\nu)/3.396] + \left(\phi + \frac{4}{\phi} \right)^2 [2.2407 \frac{EI_e}{bD} \phi^2 \end{aligned}$$

$$-(1-\nu)4.896] - (\phi + \frac{I}{\phi}) (\phi + \frac{4}{\phi}) [3.08 \frac{EI_e}{bD} \phi^2 - (1-\nu)22.5] - (1-\nu^2)23.7308$$

or, from a much simpler following formula for ψ ,

$$\phi^2 + (EI_e/bD)\phi^2 = \psi^2 [1 + (A_s/bt)] \tag{11}$$

For computing the failing stresses of panels having $\ell/\rho \geq 40$, put $m = 1$ in $\phi = m\pi b/\ell$ in the previous equations; calculate ψ and use Eq. (2) to obtain the critical stresses, which for long panels are coincident with the failing stresses of panels. Neglecting the small term ϕ^2 on the right-hand side of Eq. (11), Eq. (11) is reduced to the following simple Euler-type formula:

$$\frac{\sigma_f}{\eta} = \frac{\pi^2 EI_e}{\ell^2 (A_s + bt)} \tag{12}$$

Note that in this equation I_e is much smaller than the usual moment of inertia of cross section I_E used in the column formula. The effective moment of inertia for Z-section stiffened panels has been evaluated by the author,^{6,16} and it has the following values.

From tests done by NACA^{11,12} on Z-section stiffened panels over a wide range of variables for $\ell/\rho = 10, 17.0, 42.5$, and 62.5 , the following results are inferred. For panels having $\ell/\rho = 42.5$ with $h/t_s > 12$ and $\rho/\rho = 62.5$, $t_s/t < 0.6$, the effective moment of inertia is

$$I_e = I_s + A_s \bar{Y}_s^2 \frac{[I + \frac{1}{2}(A_s/bt)]}{[I + (A_s/bt)]^2} \tag{13}$$

For panels having $\ell/\rho = 42.5$ with $h/t_s = 12$ and $\ell/\rho = 62.5$ with $t_s/t > 0.6$,

$$I_e = I_s + \frac{A_s \bar{Y}_s^2}{(I + A_s/bt)^2} \tag{14}$$

For long buckled panels having $\ell/\rho \geq 62.5$ and $t_s/t \leq 0.63$, Eq. (13) can be used. It may be noted here that, if b/t is considerably less than h/t_s , the I_e is much smaller and could be equal to the moment of inertia I_s of the stiffener on its own.

The author, in his recent work, has shown that Eq. (13) of Ref. 6 and the present Eqs. (10) and (12) yield identical results. Hence, the most simple equation [Eq. (12)] can be used for computing the failing stresses of long panels.

Long Buckled Panels

It is known that short wave (local) buckling generally does not cause immediate failure of panels. The panels subjected to local instability are capable of carrying much higher loads after local buckling. It was shown⁶ that such panels having $\ell/\rho \geq 62.5$ fail by skin buckling in long wave, with short wave buckled skin assumed to be remaining fully effective in the long wave buckling mode. Many configurations of panels presumed to have failed in this manner are listed in Table 3 of Ref. 6. In the following, one such panel is given for illustration. The panel has the following dimensions: $t_s = 0.0642$ in. $t_s/t = 0.619$ $b/t = 59.1$ $h/t_s = 20$ $df/t_s = 807$ $d_a/t_s = 9.63$ $\ell = 22.47$ in. For this panel, short wave buckling stress = 10.7 ksi: $I_s = 0.0412$ in.⁴ $A_s \bar{Y}_s^2 = 0.076$ in.⁴ $A_s/bt = 0.244$ $\ell/\rho = 62.5$ $I_e = I_s + A_s \bar{Y}_s^2 / (I + A_s/bt)^2 = 0.0903$ in.⁴ The failing stress from Eq. (12) is 22.0 ksi, despite the much earlier local buckling of the skin. This panel, in tests,¹² failed at 21.2 ksi.

Transition Range

In the preceding, the method of determining the strength of panels having $\ell/\rho = 10$ and $\ell/\rho \geq (\ell/\rho)_t$ has been established. The remaining panel range between these limits is the transition range (Fig. 2), in which there is a considerable reliance on the use of panel tests. In fact, the major portion of the extensive NACA program on direct reading charts was concerned with test data in the transition range. However, for predicting the strength of panels in this range, empirical

Table 1 Maximum strength of 7075-T6 alloy z-stiffened panels

t_s , in.	t_s/t	b/t	h/t_s	d_f/t_s	d_A/t_s	Gerard's formula, ksi	Present theory, ksi	Test Refs. 11,12, ksi
0.0991	0.983	15.4	20.6	8.2	6.87	69.6	66.4	68.9
0.1005	0.966	20.0	20.2	8.01	6.62	65.7	67.7	70.1
0.1005	0.964	24.4	20.4	8.14	6.71	61.0	67.2	69.4
0.1024	0.998	29.6	20.0	7.87	6.78	57.0	58.0 ^a	60.0
0.1017	0.981	39.3	20.2	7.91	6.65	50.0	56.4	53.0
0.0629	0.994	50.5	20.3	8.08	7.05	44.2	48.8	46.9
0.0633	0.904	55.1	20.2	8.03	6.45	41.6	43.9	43.8
0.0642	0.943	70.9	20.2	7.93	6.67	36.6	37.6	38.0
0.0988	0.643	15.5	20.7	8.01	9.93	72.8	66.9	69.0
0.0978	0.64	20.4	21.0	8.21	10.03	63.1	66.1	69.5
0.1016	0.653	25.0	20.2	7.93	9.7	58.0	66.9	62.8
0.1018	0.656	30.3	20.0	7.94	9.58	52.4	60.0	54.8
0.1011	0.665	41.0	20.2	7.92	9.60	44.1	48.7	48.1
0.063	0.615	49.9	20.6	8.06	9.81	37.6	47.1	42.0
0.0634	0.613	59.3	20.1	8.01	9.59	33.5	42.8	39.6
0.0638	0.616	73.9	19.9	7.96	8.61	29.0	37.3	36.2
0.0986	0.406	30.1	20.1	8.11	13.18	42.4	58.9	55.2
0.0667	1.043	50.0	27.7	11.56	6.64	40.6	42.6	40.1
0.0657	0.642	50.0	29.6	11.74	9.57	35.9	37.6	38.3
0.0649	0.418	50.4	29.6	11.83	12.75	28.8	35.7	40.4
0.1037	0.609	15.1	39.3	15.53	9.75	55.8	41.2	42.2
0.1038	0.687	20.6	40.2	15.51	9.37	50.4	40.7	43.1
0.1027	0.657	25.0	40.0	15.71	9.60	46.8	40.7	43.7
0.1044	0.671	30.0	39.0	15.48	9.35	43.8	41.4	41.9
0.1025	0.673	41.2	40.1	15.90	9.6	37.4	35.7	35.9
0.0658	0.645	50.1	39.1	15.53	9.48	33.7	34.2	33.9

^aShort wave buckling.

methods have been used, most of which generally are based on a simple power law of the form

$$\sigma_f = \sigma_{m,0} - C(\ell/\rho)^n \tag{15}$$

where $\sigma_{m,0}$ is the stress at $\ell/\rho=0$, and n is the parameter that depends upon the stress at $(\ell/\rho)_{tr}$ and establishes the shape of the empirical curve. If it is assumed that the stress at $(\ell/\rho)_{tr}$ is equal to half of $\sigma_{m,0}$ and is equal to the limit of proportionality of the material of the panel, and that the tangent to the curve of Eq. (15) is equal to the tangent to the Euler parabola [Eq. (9)] at $(\ell/\rho)_{tr}$, the preceding equation becomes

$$\sigma_f = \sigma_{m,0} - \frac{\sigma_{m,0}^2}{4\pi^2 E} \left(\frac{l}{\rho}\right)^2 \tag{16}$$

This equation is known as Johnson's parabolic formula. Because the maximum strength of panels, both in theory and tests, is defined to be strength $\sigma_{m,10}$ at $\ell/\rho=10$, and since that condition of stress imposed does not hold for all of the materials and in all of the circumstances, Eq. (16) cannot be used, because it is for predicting the strength of stiffened panels in the transition range. In the following, the power law Eq. (15) is employed without any restrictions on the values of C and n , as follows.

Panels in which the Skin Does Not Buckle Locally

In order to take into account the maximum strength at $\ell/\rho = 10$, Eq. (15) is written as

$$\sigma_f = \sigma_{m,10} - C[(\ell/\rho) - 10]^n \tag{17}$$

For long panels within the limit of proportionality of the material, and up to $(\ell/P)_{tr}$, Eq. (12) is used, and is written as

$$\sigma_f = \frac{\pi^2 E}{(\ell/\rho)^2} \left(\frac{\rho_e}{\rho}\right)^2 \tag{18}$$

where

$$\rho_e = \left[\frac{I_e}{(A_s + bt)} \right]^{1/2}$$

Now assuming the condition that the tangent to the curves in Eqs. (17) and (18) and stresses obtained from these equations at $(\ell/\rho)_{tr}$ are equal, the two unknowns in Eq. (17) can be calculated. They are found to be

$$n = \frac{2\sigma_{tr}}{(\sigma_{m,10} - \sigma_{tr})} \frac{(\ell/\rho)_{tr} - 10}{(\ell/\rho)_{tr}} \tag{19}$$

and

$$C = \frac{(\sigma_{m,10} - \sigma_{tr})}{\{(\ell/\rho)_{tr} - 10\}^n} \tag{20}$$

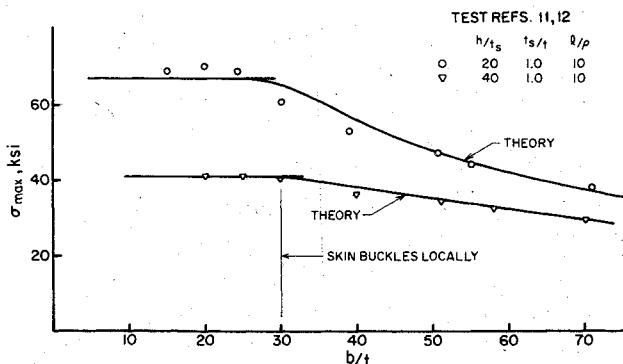


Fig. 3 Maximum strength of 7075-T6 aluminum alloy Z-stiffened panels.

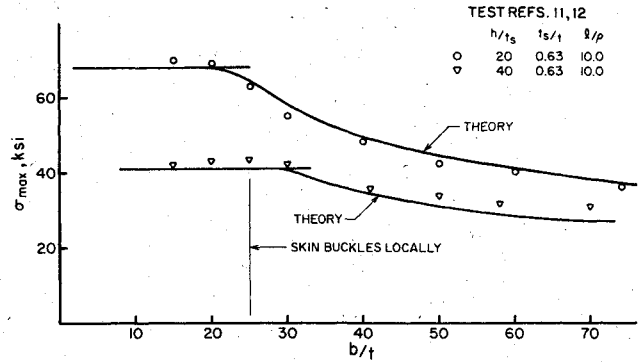


Fig. 4 Maximum strength of 7075-T6 aluminum alloy Z-stiffened panels.

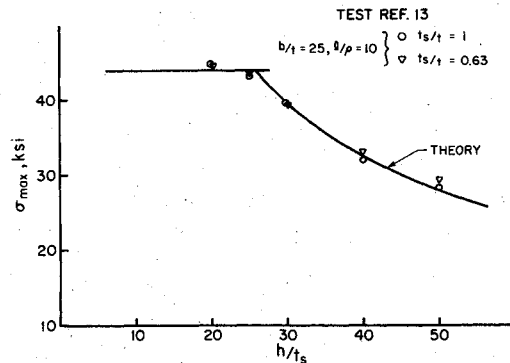


Fig. 5 Maximum strength of 24S-T aluminum alloy Z-stiffened panels.

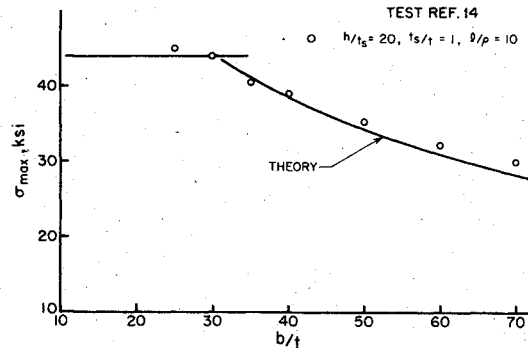


Fig. 6 Maximum strength of 24S-T aluminum alloy Z-stiffened panels.

Using these values in Eq. (18), the strength of unbuckled panels in the transition range can be determined. The method is illustrated by the following example. A 75S-T6 aluminum alloy Z-stiffened panel has the following dimensions: $t_s = 0.0997$ in $t_s/t = 0.981$ $b/t = 25.0$ $h/t_s = 20.8$ $d_f/t_s = 7.94$ $d_a/t_s = 6.63$ $2l/h = 34.3$ $\ell/\rho = 42.5$. Equation (18) is valid for unbuckled panels up to $\ell/\rho = 40$. Hence, for unbuckled panels, $(\ell/\rho)_{tr} = 42.5$ can be used.

The following values are computed: $I_e = 0.32$ in⁴, $\sigma_{tr} = 41.5$ ksi from Eq. (12) or (18). With $\sigma_{cy} = 76.9$ ksi, $\sigma_{m,10} = 68.1$ ksi from Eq. (5). From Eqs. (19) and (20), we have $n = 2.39$ and $C = 6.48$. Hence, for computing the strength of panels of the previous configuration in the transition range $10 < \ell/\rho \leq 42.5$, the following equation results

$$\sigma_f = 68100 - 6.48 [(\ell/\rho) - 10]^{2.39}$$

For $\ell/\rho = 17.5$ and 27.5 , the failing stresses from this equation are calculated, respectively, as 67.3 and 62 ksi. Test¹¹ values

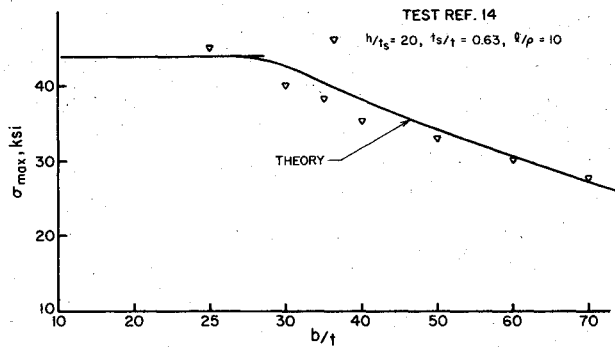


Fig. 7 Maximum strength of 24S-T aluminum alloy Z-stiffened panels.

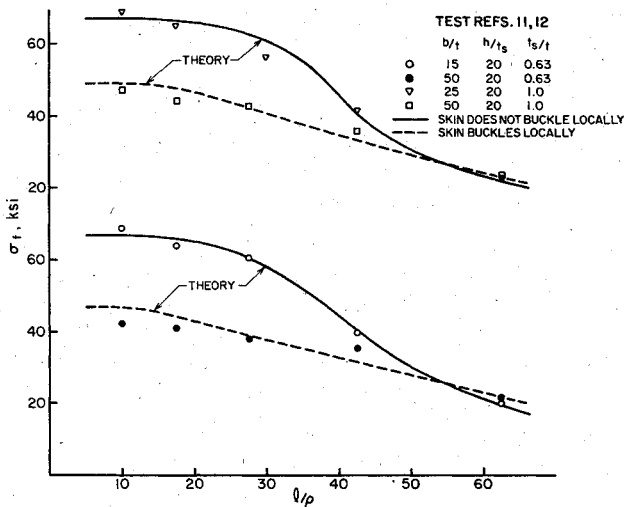


Fig. 8 Failing stresses of 7075-T6 aluminum alloy Z-stiffened panels.

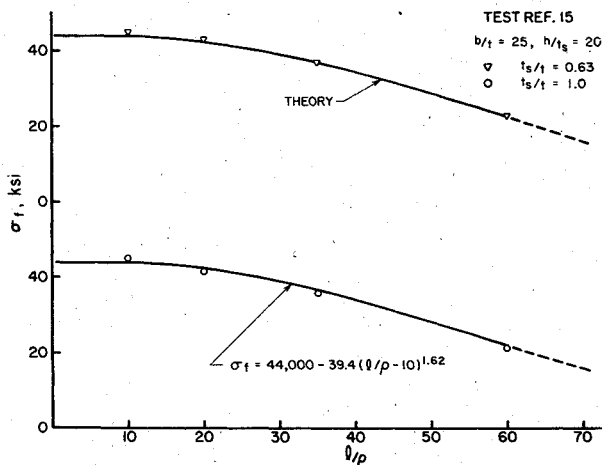


Fig. 9 Failing stresses of 24S-T aluminum alloy Z-stiffened panels.

for panels of these slenderness ratios are, respectively, 66.7 and 55.9 ksi. Note that the strength of stiffeners is assumed to be equal to the strength of panels if the skin does not buckle locally.

Buckled Panels

In Ref. 17, the method developed for buckled panels is based on Johnson's parabolic formula, Eq. (16). The following method is more general and is based on Eq. (17) with the appropriate values of C and n determined from Eqs. (19) and (20). The method is illustrated in the following manner.

Table 2 Range of dimensionless parameters of panels for which theory is compared with tests

Material	t_s/t	l/ρ	b/t	h/t_s	Refs.
75S-T6 Aluminum alloy	1.0	10	15	20	11,12
	0.63	17.5	20	40	
	...	27.5	25	...	
	...	42.5	30	...	
	...	62.5	50	...	
	55	...	
	70	...	
24S-T Aluminum alloy	1.0	10	25	20	13
	0.63	25	
	30	14
	40	
	50	
	1.0	10	25	20	
	0.63	...	30	...	
	35	...	
	40	...	
	60	...	
...	...	75	...		
1.0	10	25	20	15	
0.63	20		
...	35		
...	...	60	...		

Equation (18) is valid for early buckled long panels having $l/\rho \geq 62.5$. Hence, for such panels the transition slenderness ratio $(l/\rho)_tr = 62.5$ or 70 . For 24S-T aluminum alloy material, the yield stress is small; hence $(l/\rho)_tr$ should be 62.5 - 70 . Consider the panel that has the following dimensions: $t_s = 0.66$ in. $t_s/t = 0.43$ $b/t = 61$ $h/t_s = 29.2$ $d_f/t_s = 11.56$ $d_a/t_s = 12.56$. The following values are calculated: $I_E = 0.36$ in.⁴, $I_e = 0.329$ in.⁴. The short wave buckling stress = 9.7 ksi, $\rho = 0.465$ in.², $\sigma_{m,10} = 51.4$ ksi from Eq. (5); for $(l/\rho)_tr = 70$, $\sigma_{tr} = 18.9$ ksi. Hence $n = 0.997 \approx 1.0$ and $C = 542$. The edge stresses in the transition range $10 < (l/\rho)_tr \leq 70$ can be obtained from $\sigma_e = 51400 - 542 [(l/\rho) - 10]$. For the previous panel, we have $A_s = 0.232$ in.² $bt = 1.437$ in.² $A_s \bar{Y}_s^2 = 0.259$ in.⁴. Compute the failing stress of the panel at $l/\rho = 42.5$. From the preceding equation, the first trial value for edge stress at $l/\rho = 42.5$ is $\sigma_e = 33.8$ ksi. For panels having $l/\rho > 10$, Marguerre's formula for effective width gives better agreement with tests. Hence, $b_e t = 0.948$ in.²; for the previous edge stress with this effective area, the radius of gyration ρ' is given by

$$\rho'^2 = \frac{I}{A_s + bt} \left[I_s + \frac{A_s \bar{Y}_s^2}{I + A_s/bt} \right] = 0.292 \text{ in.}^2$$

$\therefore \rho' = 0.540$ in., $\rho'/\rho = 1.161$, $(l/\rho_e) = 42.5 / (\rho'/\rho) = 36.61$. For this effective slenderness ratio, $\rho_e = 37.0$ ksi. For this edge stress $b_e = 0.92$ in.². Hence, the failing is

$$\bar{\sigma}_f = \frac{A_s + b_e t}{A_s + bt} \sigma_e = \frac{1.152}{1.669} \times 37 \text{ ksi} = 25.5 \text{ ksi}$$

Repeating the calculation with the second trial value $\sigma_e = 37$ ksi, we have $\bar{\sigma}_f = 25.6$ ksi, compared to the test¹² value of 26.5 ksi.

Comparison of the Formulas with Experiment in the Transition and Long Panel Ranges

The comparison of the formulas and tests for short panel range is already discussed in the section related to the

maximum strength of panels. In this section, various formulas developed for computing the failing stress of panels in the transition and long panel ranges are compared with tests. The results are presented in Figs. 8-9. The dimensional parameters of the panels whose failing strengths are computed and then compared with tests are listed in Table 2. It is shown that the present analysis in all possible regions of interest, and the entire range of dimensions, is in excellent agreement with the tests.

Conclusions

The analytical methods that are comprehensive and self-sufficient for solving a variety of problems encountered in the design of Z-section stiffened panels are presented. Wherever it is necessary, these methods have been illustrated by examples in which the panels tested already have been analyzed and compared with tests. It is hoped that many simple and new results presented herein will make the art of design a little less cumbersome. An extensive comparison of the methods with tests over wide ranges of panel variables shows an excellent agreement.

References

- ¹Schuette, E. H., "Charts for the Minimum Weight Design of 24S-T Aluminum-Alloy Flat Compression Panels with Longitudinal Z-Section Stiffeners," NACA Rept. 827, 1945.
- ²Dow, N. F. and Keevil, A. S., Jr., "Direct Reading Design Charts for 24S-T Aluminum-Alloy Flat Compression Panels Having Longitudinal Formed Z-Section Stiffeners," NACA TN 1274, 1947.
- ³Hickman, W. A. and Dow, N. F., "Direct Reading Design Charts for 75S-T6 Aluminum-Alloy Panels Having Longitudinal Extruded Z-Section Stiffeners," NACA TN 2435, 1952.
- ⁴Gallaher, G. L. and Boughan, R. B., "A Method of Calculating the Compressive Strength of Z-Stiffened Panels that Develop Local Instability," NACA TN 1482, 1947.
- ⁵Dunn, L. G., "An Investigation of Sheet-Stiffened Panels Subject to Compression Loads with Particular Reference to Torsionally Weak Stiffeners," NACA TN 752, Feb. 1940.
- ⁶Yusuff, S., "Buckling Phenomena of Stiffened Panels," *Journal of Aerospace Sciences*, Aug. 1953, pp.507-514.
- ⁷Yusuff, S., "An Investigation of Short Wave Buckling of Stiffened Panels by the Energy Method," *Journal of Applied Mechanics*, Dec. 1974, pp. 1131-1133.
- ⁸Gerard, G., "Handbook of Structural Stability, Part V—Compressive Strength of Flat Stiffened Panels," NACA TN 3785, Aug. 1957.
- ⁹Gerard, G., "The Crippling Strength of Compression Elements," *Journal of the Aeronautical Sciences*, Vol. 25, Jan. 1958, pp.37-52.
- ¹⁰Boughan, R. B. and Baab, G. W., "Charts for Calculation of the Critical Compressive Stress for Local Instability of Idealized Web and T-Stiffened Panels," NACA ARR No. L4H29, Aug. 1944.
- ¹¹Hickman, W. A. and Dow, N. F., "Data on the Compressive Strength of 75S-T6 Aluminum Alloy Flat Panels with Longitudinal Extruded Z-Section Stiffeners," NACA TN 1829, Mar. 1949.
- ¹²Hickman, W. A. and Dow, N. F., "Data on the Compressive Strength of 75S-T6 Aluminum Alloy Flat Panels, Having Small, Thin, Widely Spaced Longitudinal Extruded Z-Section Stiffeners," NACA TN 1978, Nov. 1949.
- ¹³Dow, N. F. and Hickman, W. A., "Effect of Variation in Diameter and Pitch of Rivets on Compressive Strength of Panels with Z-Section Stiffeners, Panels That Fail by Local Buckling and Have Various Values of Width to Thickness Ratios for the Webs of Stiffeners," NACA TN 1737, Nov. 1948.
- ¹⁴Dow, N. F. and Hickman, W. A., "Effect of Variation in Diameter and Pitch of Rivets on Compressive Strength of Panels with Z-Section Stiffeners -Panels of Various Stiffener Spacings That Fail by Local Buckling," NACA TN 1467, Oct. 1947.
- ¹⁵Dow, N. F. and Hickman, W. A., "Effect of Variation in Diameter and Pitch of Rivets on Compressive Strength of Panels with Z-Section Stiffeners-Panels of Various Lengths with Close Stiffener Spacing," NACA TN 1421, 1947.
- ¹⁶Yusuff, S., "Design for Minimum Weight," *Aircraft Engineering*, Vol. 32, Oct. 1960, pp. 288-294.
- ¹⁷Sechler, E. E. and Dunn, L. G., *Airplane Structural Analysis and Design*, Wiley, New York, 1942.

From the AIAA Progress in Astronautics and Aeronautics Series . . .

SOLAR ACTIVITY OBSERVATIONS AND PREDICTIONS—v. 30

Edited by Patrick S. McIntosh and Murray Dryer, National Oceanic and Atmospheric Administration

The twenty-five papers in this volume present a representative view of solar-terrestrial physics, with emphasis on the sun, and on predicting solar activity affecting the space environment. It summarizes current knowledge of solar observations and theories, the interplanetary medium, geophysical responses to solar activity, and progress in the technology of forecasting such phenomena.

Solar activity variations, properties, and organization are reviewed in evaluating solar active regions and directions for further study. The structure of the solar magnetic field is explored, and current knowledge of solar flares and other activity is presented. Solar flares are modeled as an explosive release of magnetic energy associated with a current sheet in the solar magnetic field.

Interplanetary medium studies concern the solar wind and solar cosmic rays, with spacecraft observations of both. Solar activity effects on the earth's atmosphere, and relation of such activity to geomagnetic phenomena, are explored. Solar activity forecasting relates to flare activity prediction, both proton and nonproton, forecasting both incidence and solar flare location.

444 pp., 6 x 9, illus. \$12.25 Mem. \$17.50 List

TO ORDER WRITE: Publications Dept., AIAA, 1290 Avenue of the Americas, New York, N. Y. 10019